

Experimental Study and Analysis of Soft and Permanent Errors in Digital Cameras

Glenn H. Chapman, Rahul Thomas, Rohan Thomas,
School of Engineering Science
Simon Fraser University
Burnaby, B.C., Canada, V5A 1S6
glennc@ensc.sfu.ca, rmt3@sfu.ca, rohant@sfu.ca

Israel Koren, Zahava Koren
Dept. of Electrical and Computer Engineering
University of Massachusetts
Amherst, MA, 01003
koren,zkoren@ecs.umass.edu

Abstract— Digital cameras, like other digital circuits, experience hits by high-energy cosmic particles. In regular digital circuits, if the charge deposited by a particle hit happens to change the state of a flip-flop, the circuit will suffer a short lived error that is often called a *soft error* or a *single event upset* (SEU). If, on the other hand, the deposited charge propagates through the circuit without causing a state error, there will be no indication that such a hit ever occurred. The latter is often called a *single event transient* (SET). In contrast to other ICs, the CMOS Active Pixel Sensor (APS) in a digital camera can record the effect of most particle hits by displaying a pixel output that is brighter than the incoming illumination. Although in regular ICs particle hits rarely cause permanent damage, permanent defects in digital camera pixels, caused by cosmic particles, are very often observed in practice. This paper presents an experimental study of SEUs in digital cameras and compares their rate to that of SEUs in SRAM memory and to the rate of permanent defects in cameras. The analysis of SEUs in digital cameras can provide important information about the nature and distribution of particle hits and their occurrence rate, about the development of permanent defective pixels (also called “hot pixels”), and increase our understanding of SEUs in regular ICs.

Keywords- Active pixel sensor (APS), single event transients (SETs), single event upsets (SEUs), hot pixels.

I. INTRODUCTION

Digital imagers are commonly integrated in an increasing number of devices like cell phones, medical devices, and cars. As digital imager sensors are microelectronic circuits in nature, they experience, like other integrated circuits, both transient and permanent faults. The transient, short-lived, defects are called “*soft errors*” or “*single event upsets* (SEUs)” in the literature [8], and are generally believed to be caused by cosmic particles [10,11] that strike the sensor at random times and locations. As opposed to other ICs, where permanent damage caused by particle hits is rare, digital imagers are known to incur permanent defects caused by radiation, e.g., [1,10]. These permanently-defective pixels often appear soon after fabrication, and increase in number during the sensor’s lifetime. A defective pixel is almost always a “hot pixel” and results in a bright dot in the image taken by the camera, a dot

which will become brighter with a longer exposure time and/or increased sensitivity (ISO setting).

There has been a considerable number of studies of SEUs in digital ICs, e.g., [6,8,9]. Several recent publications have focused on SEUs in digital imagers [3,11], with most of them concentrating on using the imager for the characterization of cosmic particles. The latest in this direction are cell phone camera applications intended to detect cosmic ray activity from all over the world [4].

The main goal of our research, on the other hand, is not to measure the cosmic activity, but to study the decrease in image quality due to imager defects. Clearly the image quality in the presence of defects depends on the camera design parameters, and so our results can allow camera manufacturers to improve the reliability of their designs. In [2], we introduced the experimental setup we use in order to capture SEUs in digital cameras (which can easily be missed in regular camera use), and reported our initial findings. This paper presents a more rigorous analysis of the rate at which SEUs occur, and compares it to the rate of SEUs in SRAM memory.

Most cosmic particles that hit digital imagers will only cause SEUs, while very few will result in permanent defects. We wish to find the ratio between the rate of the short-lived SEUs and the rate of permanent defects. Studying SEUs in digital imagers is considerably simpler than in regular ICs. It can be done by taking dark-field photos at a high frequency and long exposure times (up to 30 sec). The instant an SEU occurs, the charge it deposits is captured as a bright dot and is retained in the image even after the SEU disappears. We devised an experiment for recording SEUs using dark-field photography, and developed software for detecting them and finding the frequency distribution of the charge that they deposit, using the brightness of the defective pixels. A different software algorithm allowed us to identify the number of permanent hot pixels existing in the camera.

The paper is organized as follows. In Section II we briefly describe “hot pixel” defects. In Section III we describe our experimental setup. Section IV presents our empirical numerical results and Section V shows how these results can be analyzed. Section VI concludes the paper.

II. HOT PIXELS

A radiation-induced defect in a pixel of a digital camera will, as a result of the charge deposited by the particle,

manifest itself in the photos taken by this camera as a point in the image being brighter than it should. This type of defective pixel is called a *hot pixel*. The pixel input and output are traditionally presented as an integer between 0 and 255, where 0 represents no illumination (black) and 255 represents saturation (white). Because of the spatial and temporal randomness of defective (SEUs or permanent) pixels occurrences, it is accepted among researchers that they are, in fact, caused by a source that is random by nature, most likely cosmic particles [1,10].

III. EXPERIMENTAL SETUP

In order to quantify rates of SEUs and permanent hot pixels in cameras, we used dark-field photography, as it easier to identify a bright dot on an otherwise totally black background. Our first test devices were APS (CMOS) Digital Single Lens Reflex (DSLR) cameras. DSLRs have a large sensor area with highly sensitive pixels, and allow direct access to the RAW pixel values. RAW images contain the pixel data as taken by the camera and are not processed by algorithms such as jpeg or demosaicing. We used in our experiments three different DSLR cameras, listed in Table 1.

TABLE 1: The three cameras studied in this paper.

	Camera model	No. of pixels	Pixel size	Sensor area
1	Canon 5DSR	50.6M	4.14 μ	864 mm ²
2	Canon 5DmarkII	21.1M	6.26 μ	836 mm ²
3	Canon T1i	15.1 M	4.69 μ	332 mm ²

With each camera, we took a series of medium to long exposures at a fixed ISO. Because the exposure time for each image was fixed, we could look for events that occur only in a single image and then go away. The key point is that SEUs are, by their nature, very short in duration and inject a charge into a small local area of the IC. However, in digital imagers, the pixel integrates the charge over the duration of the exposure, and by taking an exposure of a given duration the imager records both the temporal and spatial occurrence of each SEU even if the SEU disappears before the exposure ends. Still, we could not take very long exposures as the camera accumulates noise in the image (e.g., thermal generated electrons) over time. The maximum exposure time varies with the camera and the ISO, but is typically in the order of 10 to 30 seconds before noise becomes so prevalent that differentiating between SEUs and noise is difficult. Therefore, in our experiments we took a sequence of short duration images, no longer than 30 seconds.

In order to efficiently measure the effect of SEUs on imagers for various operating conditions, we created an experimental setup to collect a large number of dark-frame images. These images need to be precise temporal snapshots of the sensor activity for a specific time period at given ISO levels and exposure times. The sequence of images also allowed us to separate SEUs from permanent hot pixel events and obtain temporal rates for these two different events.

To take multiple shots at a fixed ISO and exposure time, we used a digital camera remote control, called an intervalometer, which can take continuously a sequence of

images. The experiment was set up such that after each shot (image), a one-minute delay was inserted allowing the camera to cool down between shoots, to remove any effects of thermal noise caused by the sensor heating up as the experiment progressed. On average, a set of 100 images was collected for each ISO and exposure time combination. The 100-image limit was also influenced by the maximum storage capacity of the internal SD card and the picture limit of the camera batteries. We conducted this experiment for three ISO settings, namely ISO 1600, 3200 and 6400, and four exposure times – 30 seconds, 10 seconds, 3.2 seconds, and 1 second. These experiments were repeated for the three cameras described in Table 1. These experiments were all conducted in a pitch-dark room with the lens cap on, so that no incident light fell onto the camera sensor. This enabled us to detect any defect caused by SEUs or permanent hot pixels.

To analyze the images for potential defective pixels, we developed a software tool that reads in the RAW image data and then executes the following 4-step algorithm using three consecutive images at a time: (1) Flag any pixel that has an increase in value from image j to image $j+1$ using a predetermined threshold. (2) Using the pixel locations from the previous step, check to see if any of them has a decrease in pixel value from image $j+1$ to image $j+2$ using the same predetermined threshold. (3) If any pixel location satisfies the above conditions, it is marked as an SEU defect location and its response (brightness) is recorded. (4) If the location has at least two out of the three values above the threshold, it is marked as a permanent hot pixel.

IV. EXPERIMENTAL RESULTS

Using the detection algorithm mentioned in the previous section, we have discovered several interesting forms of SEU defects. An example of an SEU streak is shown in Figure 1.

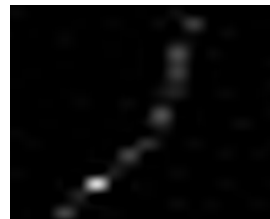


Figure 1: A simple SEU Streak (snapshot of 5x5 pixels in size) Figure 2: A complex SEU Streak (snapshot of 12x17 pixels)

In this figure, an incident cosmic ray has hit the imager at a low angle, depositing a charge covering three neighboring pixels in a line. We consider this as a single SEU since the cause of this streak is likely a single particle hit. We justify this by noting that the event rate (at most a few SEUs per a 21 megapixel image) is such that the probability of three events occurring at neighboring pixels is negligible. These streaks are similar to the trails left by cosmic ray particles in cloud chamber detectors. A more complicated streak is shown in Figure 2. In this example, it is clear that the incident cosmic particle began at a particular direction, but at some point it incurred a deflection. One possibility is that the incident cosmic particle collided with an atom, causing the particle to deflect and create this interesting image. We considered such a streak a single SEU, in spite of the gaps.

We gathered the data for each camera separately, in order to see whether the camera’s age or design parameters (e.g.,

sensor area or pixel area) have an impact on defect development. For each SEU, we calculated its charge by multiplying the defective pixel's brightness (between 0 and 255) by the number of electrons needed to increase this luminosity by 1. In case of a cluster of bright pixels, we added the luminosities of all pixels in the cluster to get the charge of what we consider a single SEU. We then calculated, for each camera, the frequency distribution of the SEU charges, the total number of SEUs, and the number of hot pixels.

V. ANALYSIS OF RESULTS

Using the data obtained by our experiments, we can attempt to identify certain trends and rates of defect growth at various operating conditions of the imager. For a more rigorous analysis of these results, we fit a two-parameter Weibull distribution to the empirical data [6]. The Weibull probability density function is given by

$$f(x; \alpha, \beta) = (\alpha / \beta)(x / \beta)^{\alpha-1} \exp(-(x / \beta)^\alpha) \quad (1)$$

where x is the charge in electrons, α is the shape parameter and β is the scale parameter of the distribution. The Weibull cumulative distribution function, F , is shown in Equation (2)

$$F(x; \alpha, \beta) = 1 - \exp(-(x / \beta)^\alpha) \quad (2)$$

Because x is continuous while the actual measured charge assumes discrete values, we based our curve fitting on Equation (3), where C denotes the discretized charge value (as opposed to the continuous x) and Δ is the granularity of the measured deposited charge (e.g., $\Delta=78.1e$ for camera 1),

$$\text{Prob}(C = c) = F(c + 0.5\Delta) - F(c - 0.5\Delta) \quad (3)$$

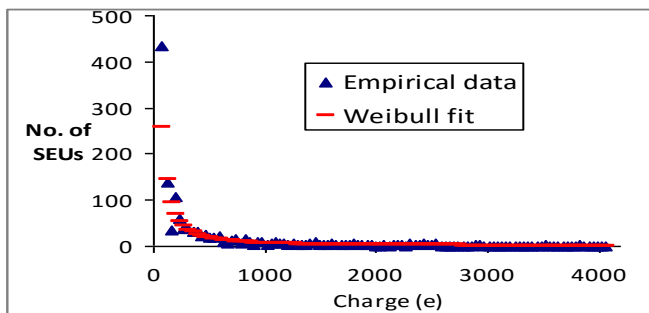


Figure 3: Frequency distribution of charge for camera 1.

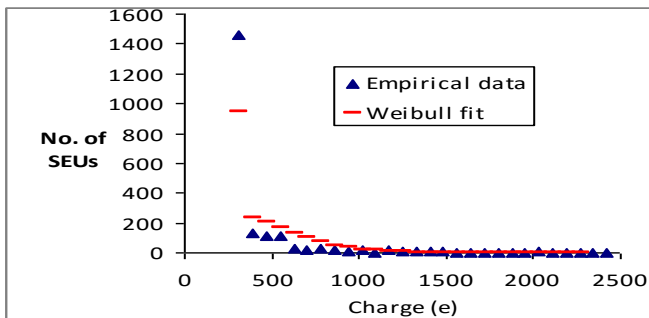


Figure 4: Frequency distribution of charge for camera 2.

Figures 3 and 4 show the empirical frequency distribution of the charge (in electrons (e)), for cameras 1 and 2,

respectively, as well as the best fitting Weibull-predicted frequencies based on Equation (3). The figure for camera 3 is omitted for brevity. In all 3 cases, we obtained an excellent fit between the analytic equation and the empirical results. The values of the parameters for the three cameras, obtained by using the Method of Moments estimation, are summarized in Table 2. R^2 measures the goodness of fit between the Weibull distribution and the empirical distribution.

Table 2: The Weibull fit parameters for the three cameras.

Camera	α	β	R^2
1	0.707	378.7	0.9682
2	1.658	459.6	0.9365
3	0.700	286.7	0.9437

Because our empirical results depicted in Figures 3 and 4 pertain to different experiment durations and different sensor areas, they cannot be easily compared, let alone be compared to the SEU rates of other ICs. We would like to define a *normalized rate* of SEUs for each charge, so that a fair comparison can be made between the different ICs. More specifically, we would like to compare the rate of SEUs per charge of our 3 cameras to that of SRAM cells quoted in the literature. This normalized rate will also be useful for comparing camera SEU rates to permanent hot pixel defects rates.

We denote this normalized rate by $\lambda(c)$ and define it as *the expected number of SEUs with charge c per year, per mm^2 of the specific IC*. To calculate $\lambda(c)$ for the three cameras in the study, we denote by A the sensor area of the camera (in mm^2), by T the total exposure time of this camera (in seconds), and by N the total number of SEUs recorded in our experiments for this camera, and then define

$$\lambda(c) = \frac{N \times \text{Prob}(C = c)}{A \times T} \times 3.15 \cdot 10^7 \quad (4)$$

$\text{Prob}(C=c)$ is defined in Equation (3) and $3.15 \cdot 10^7$ is the number of seconds in a year. Using the values of N , A , and T listed in Table 3, we can now calculate $\lambda(c)$ for each of the 3 cameras to obtain a fair comparison for the different ICs.

Table 3: Total number of SEUs (N), Sensor area (A), and Total exposure time (T) for the three cameras.

Camera	N	A (mm^2)	T (seconds)
1	1295	864	16,500
2	1997	864	19,300
3	387	332	9,150

Figure 5 compares the normalized distribution $\lambda(c)$ for the three cameras based on Equation (4) and Table 3. We can see that the curves for the two cameras with the smaller pixel sizes are very close while the curve for camera 2 with the larger pixel size is different, demonstrating the impact of the pixel size.

We next compare the SEU rates in digital cameras to those in SRAM arrays, as SRAMs have a regular structure similar to the camera sensor, and are the digital circuits that are the most sensitive to particle hits. Based on [7], the amount of charge needed for a particle hit to generate a noticeable SEU in a standard SRAM is greater than or equal to 0.4 fCoulomb, which is equal to 2500e.

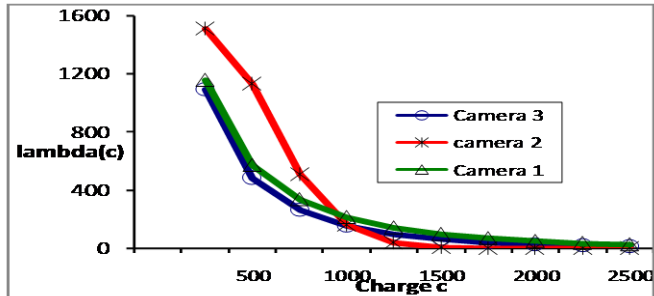


Figure 5: Normalized SEU rate $\lambda(c)$ as a function of the charge for the three cameras.

To obtain the camera cumulative SEU rate for a charge that is equal to or greater than a given charge c , a rate which we denote by $\Gamma(c)$, we need to add up the individual rates λ ,

$$\Gamma(c) = \sum_{i \geq c} \lambda(i).$$

For $c=2500e$, the calculated value of $\Gamma(2500)$ for the three cameras is in the range [43.4,93.5]. The reported SEU rates for SRAM cells are in the range of [200,5000] FIT/1Mbit [5]. As the area of an SRAM cell is about $0.1\mu\text{m}^2$, the corresponding normalized rate (in number of SEUs per $\text{mm}^2\cdot\text{year}$) is in the range [1.75,43.0]. Thus, the observed range of rates for digital cameras is somewhat higher than the range for SRAM, but is in the same order of magnitude.

For the three cameras in our experiments, between 1% and 2% of the SEUs (based on the Weibull fit) have a charge that is equal to or larger than 2500e. In other words, only about 1% out of the particle hits that are observed and recorded by the camera will cause an SEU in SRAM.

When attempting to compare the camera SEU rate to the permanent hot pixels rate, we must be aware that the charge that caused the hot pixel cannot be measured once the hot pixel is already present. Therefore, we cannot compare the charge-specific rates but only the overall rates. The overall SEU rate over all charges is $\sigma = \sum_{c \geq 1} \lambda(c)$. Because hot pixels

accumulate during the whole life of the camera, we calculated their normalized rate as the current number of hot pixels in the camera, divided by the sensor area (in mm^2) and by the age of the camera (in years). The observed rates for the three cameras in our study were in the range [0.066,0.095] per $\text{mm}^2\cdot\text{year}$, while the calculated total SEU rates σ are in the range [2287,3361] per $\text{mm}^2\cdot\text{year}$. We conclude that SEUs in digital cameras are from 24,000 to 51,000 more common than the permanent hot pixels. By comparison, for ordinary ICs the literature indicates that SEUs are about 100 times more common than permanent faults. This much higher rate in digital imagers is the result of the considerably higher sensitivity of pixels to injected charges. However, it may also be that imagers are recording other cosmic particles, such as muons, that do not affect regular digital circuits.

VI. CONCLUSIONS

This paper has presented the results of an experimental study that focused on SEUs and permanent defects in digital cameras. We showed that SEU rates can be modeled using a Weibull distribution, which allowed us to estimate the rate of high charge particle hits that may result in an SEU in an SRAM memory cell, and compare it to the SRAM SEU rate mentioned in the literature. As SEUs are easily detectable in digital imagers, we plan on further studying their rates as a function of the camera parameters such as pixel size and sensitivity (ISO), and at higher altitudes rather than at sea level only. Such a study can prove to be useful for both camera manufactures and regular ICs manufacturers.

Acknowledgments: The authors wish to thank Klinsmann J. Coelho Silva Meneses and Tommy Q. Yang for their help in performing some of the early experiments in this project.

REFERENCES

- [1] G.H. Chapman, I. Koren and Z. Koren, "Do More Camera Pixels Result in a Better Picture?" *Proc. IEEE 18th International On-Line Testing Symposium (IOLTS)*, pp. 75-78, June 2012.
- [2] G.H. Chapman, R. Thomas, R. Thomas, K. Meneses, T. Yang, I. Koren, and Z. Koren, "Single Event Upsets and Hot Pixels in Digital Imagers," *Proc. 2015 Intern. Symposium on Defect and Fault Tolerance in VLSI*, pp. 41-46, Oct. 2015.
- [3] A. Chugg, R. Jones, M. Moutrie, C. Dyer, K. Ryden, P. Truscott, J. Armstrong, and D. King, "Analyses of CCD images of nucleon-silicon interaction events," *IEEE Trans. Nucl. Sci.*, vol. 51, pp. 2851-2856, 2004.
- [4] Deco. [Online]. Available: <http://wipac.wisc.edu/deco>
- [5] F. Faccio, K. Kloukinas, G. Magazzù, and A. Marchioro, "SEU effects in registers and in a Dual-Ported Static RAM designed in a $0.25\mu\text{m}$ CMOS technology for applications in the LHC," *Fifth Workshop on Electronics for LHC Experiments*, September 1999, pp. 57-124.
- [6] F. Firouzi, M. Salehi, F. Wang, and S-M. Fakhraie, "An accurate model for soft error rate estimation considering dynamic voltage and frequency scaling effects," *Microelectronics Reliability*, 2011.
- [7] L. Kou, "Impact of Process Variations on Soft Error Sensitivity of 32-nM VLSI Circuits in Near-Threshold Region," PhD Dissertation, Vanderbilt University, May 2014.
- [8] S. Mitra, T. Karnik, N. Seifert, and M. Zhang, "Logic soft errors in sub-65nm technologies design and CAD challenges," *Proc. of the 42nd Design Automation Conference, DAC '05*, 2005, pp. 2-4.
- [9] S. Mukherjee, *Architecture Design for Soft Errors*, Elsevier, Inc., 2008.
- [10] A.J.P. Theuwissen, "Influence of terrestrial cosmic rays on the reliability of CCD image sensors. Part 2: experiments at elevated temperature," *IEEE Transactions on Electron Devices*, Vol. 55 (9), pp. 2324-8, 2008.
- [11] Z. Török and S. P. Platt, "Application of imaging systems to characterization of single-event effects in high-energy neutron environments," *IEEE Trans. Nucl. Sci.*, vol. 53, pp. 3718-3725, 2006.